

Fluorescein Provides a Resonance Gate for FRET from Conjugated Polymers to DNA Intercalated Dyes

Shu Wang, Brent S. Gaylord, and Guillermo C. Bazan*

Contribution from the Departments of Chemistry and Materials, Institute for Polymers and Organic Solids, University of California, Santa Barbara, California 93106

Received April 9, 2003; E-mail: bazan@chem.ucsb.edu

Abstract: Fluorescence spectra show that excitation of the cationic water-soluble conjugated polymer poly- $\{(1,4\text{-phenylene})\text{-}2,7\text{-}[9,9\text{-bis}(6'\text{-}N,N,N\text{-trimethylammonium})\text{-hexyl}]\text{fluorene diiodide}\}$ (**1**) results in inefficient fluorescence resonance energy transfer (FRET) to ethidium bromide (EB) intercalated within double-stranded DNA (dsDNA). When fluorescein (FI) is attached to one terminus of the dsDNA, there is efficient FRET from **1** through FI to EB. The cascading energy-transfer process was examined mechanistically via fluorescence decay kinetics and fluorescence anisotropy measurements. These experiments show that the proximity and conformational freedom of FI provide a FRET gate to dyes intercalated within DNA which are optically amplified by the properties of the conjugated polymer. The overall process provides a substantial improvement over previous homogeneous conjugated polymer based DNA sensors, namely, in the form of improved selectivity.

Introduction

Methods for DNA detection are important to disease diagnosis, for gene-targeted drugs, and as general molecular biology tools.^{1–3} Most available methods involve hybridization of target DNA with a specific base sequence labeled with a radioisotope or a fluorophore.^{4,5} Because the detection signals generated by these methods lack amplification, one needs to rely on polymerase chain reaction (PCR) protocols to increase the concentration of specific nucleic acid sequences to detectable levels.^{6,7} Signal-amplification systems have been developed in response to this limitation, which include the use of fluorogenic substrate active enzymes,^{8,9} modified liposomes,¹⁰ and Au nanoparticles.^{11,12} Complex instrumentation, specific reagents, and non-

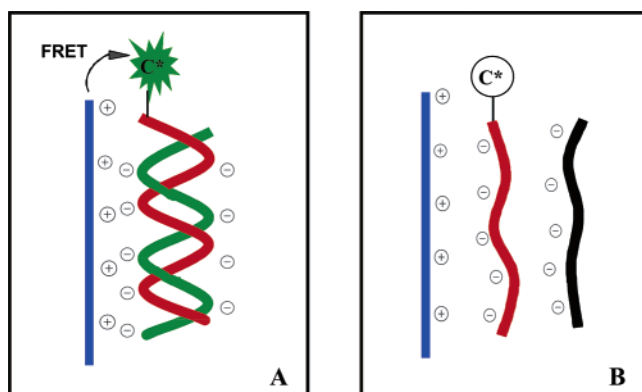
real-time testing, however, pose challenges for their practical implementation.

Homogeneous DNA hybridization assays based on fluorescence resonance energy transfer (FRET) between energy-/electron-transfer chromophore pairs are attractive because of their simplicity of operation and use of standard optical equipment.^{13,14} Recently, we reported a DNA sensor in which water-soluble conjugated polymers enhance the signals of fluorophore-modified peptide nucleic acids (PNA) and DNA strands.¹⁵ In these systems the conjugated polymer behaves as a light-harvesting unit which transfers excitations via FRET to a signaling fluorophore. When using single-stranded DNA (ssDNA) labeled with a chromophore (C*) as the probe, one encounters the two situations illustrated in Scheme 1. Scheme 1A shows the situation when the probe ssDNA-C* (shown in red) finds a complementary ssDNA (shown in green). Because the dsDNA-C* (dsDNA: double-stranded DNA) is negatively charged, electrostatic interactions bring it into close proximity to the cationic water-soluble conjugated polymer (CCP, shown in blue).^{16,17} The optical properties of the energy-transfer pair can be chosen for selective excitation of the CCP and for overlap between the CCP emission and the absorption of C* (a FRET

- (1) (a) Wang, J.; Jiang, M. *J. Am. Chem. Soc.* **1998**, *120*, 8281. (b) Xu, X. H.; Bard, A. J. *J. Am. Chem. Soc.* **1995**, *117*, 2627.
- (2) (a) Peterlinz, K.; Georgiadis, R.; Herne, T.; Tarlov, M. *J. Am. Chem. Soc.* **1997**, *119*, 3401. (b) Schork, N. J.; Fallin, D.; Lanchbury, J. S. *Clin. Genet.* **2000**, *58*, 250.
- (3) Balakin, K. V.; Korshun, V. A.; Mikhalev, I. I.; Maleev, G. V.; Malakhov, A. D.; Prokhorenko, I. A.; Berlin, Y. A. *Biosens. Bioelectron.* **1998**, *13*, 771.
- (4) (a) Demidov, V. V. *Trends Biotechnol.* **2003**, *21*, 4. (b) Bier, F. F.; Kleinjung, F. *Fresenius J. Anal. Chem.* **2001**, *371*, 151. (c) Zhai, J.; Cui, H.; Yang, R. *Biotechnol. Adv.* **1997**, *15*, 43.
- (5) (a) Whitcombe, D.; Theaker, J.; Guy, S. P.; Brown, T.; Little, S. *Nat. Biotechnol.* **1999**, *17*, 804. (b) Jenkins, Y.; Barton, J. K. *J. Am. Chem. Soc.* **1992**, *114*, 8736.
- (6) (a) Chehab, F. F.; Kan, Y. W. *Proc. Natl. Acad. Sci. U.S.A.* **1989**, *86*, 9178. (b) Nuovo, G. J. *Methods Mol. Biol.* **2000**, *123*, 217.
- (7) (a) Saiki, R. K.; Scharf, S.; Faloona, F.; Mullis, K.; Horn, G. T.; Erlich, H. A.; Arnheim, N. *Science* **1985**, *230*, 1350. (b) Lee, M. A.; Siddle, A. L.; Page, R. H. *Anal. Chim. Acta* **2002**, *457*, 61.
- (8) (a) Patolsky, F.; Katz, E.; Willner, I. *Angew. Chem., Int. Ed. Engl.* **2002**, *41*, 3398. (b) Bardea, A.; Patolsky, F.; Dagan, A.; Willner, I. *Chem. Commun.* **1999**, 21.
- (9) Saghatelian, A.; Guckian, K. M.; Thayer, D. A.; Ghadiri, M. R. *J. Am. Chem. Soc.* **2003**, *125*, 344.
- (10) Patolsky, F.; Lichtenstein, A.; Willner, I. *J. Am. Chem. Soc.* **2001**, *123*, 5194.
- (11) (a) Taton, T. A.; Mirkin, C. A.; Letsinger, R. L. *Science* **2000**, *289*, 1757. (b) Taton, T. A.; Lu, G.; Mirkin, C. A. *J. Am. Chem. Soc.* **2002**, *124*, 11248.
- (12) Su, X.; Li, S. F. Y.; O'Shea, S. J. *Chem. Commun.* **2001**, 755.

- (13) (a) Takakusa, H.; Kikuchi, K.; Urano, Y.; Sakamoto, S.; Yamaguchi, K.; Nagano, T. *J. Am. Chem. Soc.* **2002**, *124*, 1653. (b) Johansson, M. K.; Fidler, H.; Dick, D.; Cook, R. M. *J. Am. Chem. Soc.* **2002**, *124*, 6950.
- (14) Didenko, V. V. *BioTechniques* **2001**, *31*, 1106.
- (15) (a) Gaylord, B. S.; Heeger, A. J.; Bazan, G. C. *Proc. Natl. Acad. Sci. U.S.A.* **2002**, *99*, 10954. (b) Gaylord, B. S.; Heeger, A. J.; Bazan, G. C. *J. Am. Chem. Soc.* **2003**, *125*, 896. (c) Liu, B.; Gaylord, B. S.; Wang, S.; Bazan, G. C. *J. Am. Chem. Soc.* **2003**, *125*, 6705.
- (16) (a) Kabanov, A. V.; Felgner, P.; Seymour, L. W. *Self-Assembling Complexes for Gene Delivery: From Laboratory to Clinical Trial*; John Wiley: Chichester, U.K., 1998. (b) Gössl, I.; Shu, L.; Schlüter, A. D.; Rabe, J. P. *J. Am. Chem. Soc.* **2002**, *124*, 6860.
- (17) (a) Wang, Y.; Dubin, P. L.; Zhang, H. *Langmuir* **2001**, *17*, 1670. (b) Bronich, T. K.; Nguyen, H. K.; Eisenberg, A.; Kabanov, A. V. *J. Am. Chem. Soc.* **2000**, *122*, 8339.

Scheme 1



requirement).^{18,19} Combining the distance control by electrostatic interactions and the optical properties of the interacting partners gives rise to efficient FRET. Furthermore, that the emission of C* by FRET from a CCP is considerably more intense than that obtained by direct excitation at the absorption maximum of C* demonstrates the optical amplification provided by the light-harvesting properties of the CCP.²⁰ When a noncomplementary ssDNA (shown in black) is present, Scheme 1B, there is no hybridization with ssDNA-C* and there is competition between the unhybridized strands for sites adjacent to the CCP. FRET is less effective, and one can thus distinguish complementary and noncomplementary strands by examination of the C* intensity.

Despite the simplicity of the CCP assay, the screening of the noncomplementary strand is not complete and a small amount of FRET to the ssDNA-C* takes place. Residual emission limits the ability to discriminate complementary from noncomplementary DNA target sequences. These complications can be circumvented when one uses a neutral ssPNA-C* as the recognition strand since it does not bind electrostatically to the CCP in the presence of noncomplementary ssDNA.^{15a} Nonetheless, there are advantages in using labeled DNA instead of PNA, as DNA is more straightforward to prepare and DNA/DNA interactions are better understood than corresponding PNA/DNA interactions. It seemed plausible that the selectivity in a ssDNA-based assay could be improved by FRET to an intercalated dye that is emissive only upon strand-specific DNA hybridization. In this contribution we not only show that this concept is effective but provide mechanistic insight into the process by which excitations are transferred from a CCP to an intercalated DNA dye.

Results and Discussion

Ethidium bromide (EB) intercalates within the internally stacked bases of dsDNA, resulting in an increase in its fluorescence quantum yield.²¹ Our initial efforts concerned FRET experiments to EB upon excitation of a CCP. Molecular structures of the participating reagents are shown in Figure 1,

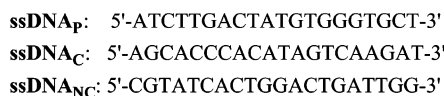
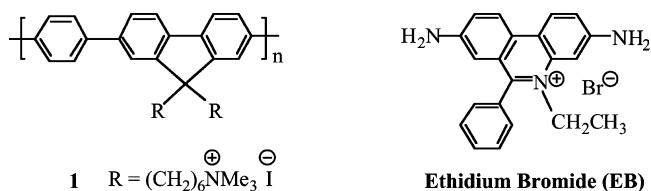


Figure 1. Chemical structures of 1, EB, and the ssDNAs.

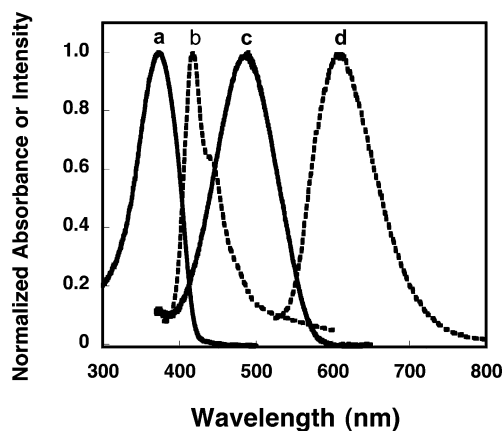


Figure 2. Absorption and fluorescence spectra of 1 (abs, a; em, b) and EB/dsDNA (ssDNA_P + ssDNA_C) (abs, c; em, d) in potassium phosphate–sodium hydroxide buffer solution (50 mM, pH = 7.40).

and relevant absorption and emission spectra are given in Figure 2. Three ssDNA sequences are given: ssDNA_P corresponds to the probe strand, ssDNA_C is a strand complementary to ssDNA_P, and ssDNA_{NC} is a strand that is not complementary to ssDNA_P. Poly{[1,4-phenylene]-2,7-[9,9-bis(6'-N,N,N-trimethylammonium)hexyl]fluorene diiodide} (1), with a molecular weight of 8,600,²² was chosen as the CCP because its emission overlaps the absorption band of EB. The spectra in Figure 2 were collected in a potassium phosphate–sodium hydroxide buffer at concentrations used in DNA hybridization protocols.²³

Our initial strategy for CCP-sensitized EB emission is illustrated in Scheme 2. A mixture of 1, EB, and ssDNA_P is mixed with an unknown ssDNA target. If the two ssDNAs are complementary (Scheme 2A), DNA duplex formation would ensue, EB would intercalate within the dsDNA, and electrostatic forces would bring the dsDNA/EB macromolecule within close proximity of the CCP. One would anticipate detecting EB emission upon FRET sensitization from the CCP. If the target ssDNA is not complementary (Scheme 2B), the formation of the dsDNA structure required for EB intercalation would not take place and no FRET to EB would be detectable. Note that EB is cationic, and electrostatic repulsion with the CCP is to be expected.

As shown by Förster,^{19b} dipole–dipole interactions lead to long-range resonance energy transfer from a donor chromophore to an acceptor chromophore. The rate constant for energy

(18) Lakowicz, J. R. *Principles of Fluorescence Spectroscopy*; Kluwer Academic/Plenum Publishers: New York, 1999.

(19) (a) Dogariu, A.; Gupta, R.; Heeger, A. J.; Wang, H. *Synth. Met.* **1999**, *100*, 95. (b) Förster, T. *Ann. Phys.* **1948**, *2*, 55.

(20) (a) McQuade, D. T.; Hegedus, A. H.; Swager, T. M. *J. Am. Chem. Soc.* **2000**, *122*, 12389. (b) Yang, J. S.; Swager, T. M. *J. Am. Chem. Soc.* **1998**, *120*, 11864.

(21) (a) LePecq, J. B.; Paoletti, C. *J. Mol. Biol.* **1967**, *27*, 87. (b) Morgan, A. R.; Pulleyblank, D. E. *Biochem. Biophys. Res. Commun.* **1974**, *61*, 346. (c) Birnboim, H. C.; Jevcak, J. *J. Cancer Res.* **1981**, *41*, 1889.

(22) (a) Stork, M.; Gaylord, B. S.; Heeger, A. J.; Bazan, G. C. *Adv. Mater.* **2002**, *14*, 361. (b) Wang, S.; Liu, B.; Gaylord, B. S.; Bazan, G. C. *Adv. Funct. Mater.* **2003**, *13*, 463.

(23) Harwood, A. J. *Basic DNA and RNA Protocols*; Humana Press: Totowa, NJ, 1996.

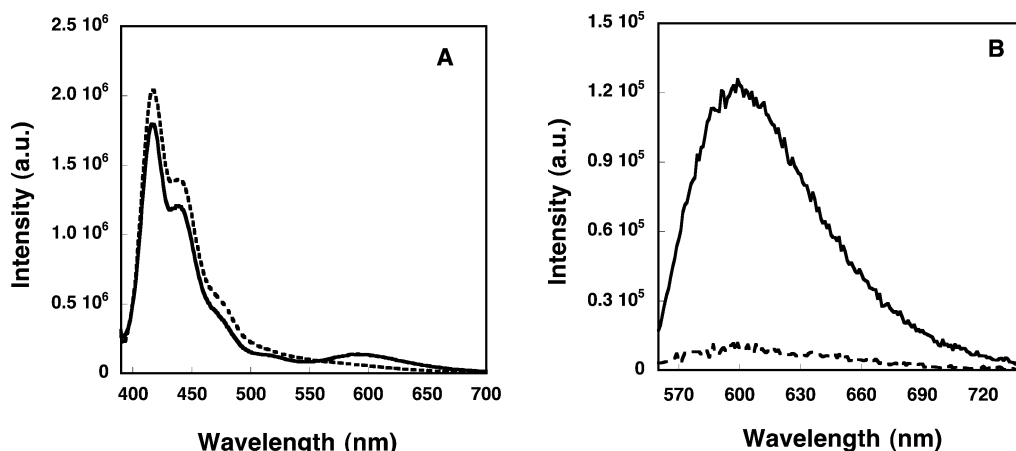
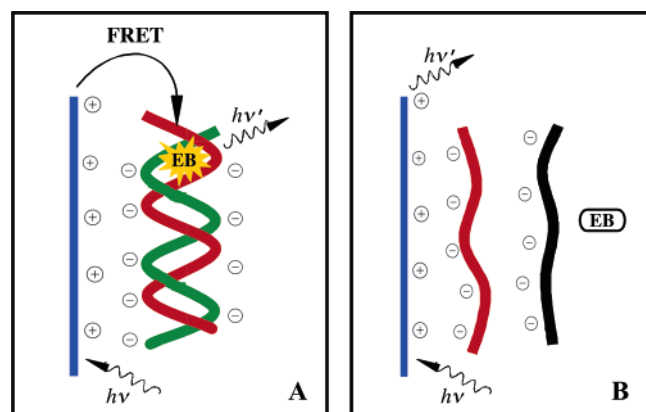


Figure 3. Emission spectra from solutions containing (solid line) **1**/dsDNA(ssDNA_P + ssDNA_C)/EB and (dotted line) **1**/ssDNA_P + ssDNA_{NC}/EB: $\lambda_{\text{ex}} = 380$ nm; $[\mathbf{1}] = 1.6 \times 10^{-7}$ M in RUs; [dsDNA, ssDNA_P, or ssDNA_{NC}] = 1.0×10^{-8} M; [EB] = 1.1×10^{-6} M. Measurements are in potassium phosphate–sodium hydroxide buffer solution (50 mM, pH = 7.40). (A) Emission spectra in the 400–700 nm range; (B) emission spectra in the EB region, with subtraction from the residual emission from **1**.

Scheme 2



transfer (k_{tr}) is dependent on the donor–acceptor distance (r), the orientation factor (κ) and the overlap integral (J), as shown in

$$k_{tr} \propto \frac{1}{r^6} \kappa^2 J(\lambda) \quad (1)$$

$$J(\lambda) = \int_0^\infty F_D(\lambda) \epsilon_A(\lambda) \lambda^4 d\lambda$$

We note that if **1** and EB are the donor and acceptor, respectively, the distance requirement for energy transfer will be controlled by the interactions in Scheme 2. The overlap integral provides the analytical expression for how the spectral overlap between the emission of the donor and the absorption of the acceptor influence the rate of transfer. As shown by Figure 2, the molecular components of the assay have been chosen to satisfy these optical requirements.

Figure 3A shows the emission spectra obtained from solutions of complementary (ssDNA_P + ssDNA_C) and noncomplementary (ssDNA_P + ssDNA_{NC}) DNA strands in the presence of **1** and EB. Hybridization was confirmed using standard absorption measurements,^{15b} and the excitation wavelength was chosen near the absorbance maximum of **1** (380 nm), where no significant EB absorption occurs (see Figure 1). Addition of EB and **1** ([EB] = 1.1×10^{-6} M and $[\mathbf{1}] = 1.6 \times 10^{-7}$ M, based on the concentration of polymer repeat units, RUs) to the DNA

solutions containing dsDNA (ssDNA_P + ssDNA_C) or ssDNA_P + ssDNA_{NC} ([dsDNA] = [ssDNA_P] = [ssDNA_{NC}] = 1.0×10^{-8} M) and subsequent comparison of the resulting fluorescence reveals EB emission predominantly when in the presence of dsDNA. Figure 3B shows that when focusing on the changes in the emission intensity of the EB, the effect of hybridization is substantial.²⁴

The FRET efficiency in Figure 3 is not high, especially when compared to previously reported studies with CCPs and fluorescein-labeled DNA and PNA.¹⁵ We suspect that the low efficiency is due to the distance (r) and orientation relationships (κ^2) which are found in eq 1.²⁵ One possibility is that charge alignment along the dsDNA and **1** leads to a nonoptimal (orthogonal) orientation between the transition moment of the conjugated backbone and that of the intercalated EB. Overall, the data in Figure 3 show that, as a sensor scheme, this fluorescence-based assay can discriminate ssDNA from dsDNA, but it is not very sensitive; the EB emission is not significantly amplified by FRET from the CCP.

On the basis of the possibility that the low FRET efficiency is the result of nonoptimized transition dipole alignment, we introduced a ssDNA_P strand with a fluorescein (FI) attached at the 5' terminus (ssDNA_P-FI). Fluorescein, with an absorption maximum at 488 nm and an emission maximum at 518 nm, was chosen since its absorption overlaps the emission of **1**¹⁸ and because its bioconjugate chemistry with DNA is well-developed.²⁶ Additionally, based on previous studies,¹⁵ it is known that FRET from **1** to FI-labeled DNA is efficient, perhaps because the FI is located at one terminus of DNA and has the freedom to sample a wider range of orientations. We also note that the emission of FI is blue-shifted (84 nm) relative to that of EB. FRET from **1** to FI, followed by a second FRET to EB, becomes energetically feasible.^{27–29}

(24) The emission of the acceptor chromophore was corrected by subtracting a normalized spectra of the donor in the absence of the acceptor.

(25) (a) Mergny, J. L.; Garestier, T.; Rougée, M.; Lebedev, A.; Chassignol, M.; Thuong, N. T.; Hélène, C. *Biochemistry* **1994**, *33*, 15321. (b) Shinozuka, K.; Seto, Y.; Sawai, H. *J. Chem. Soc., Chem. Commun.* **1994**, 1377.

(26) (a) <http://www.probes.com>. (b) Hermanson, G. T. *Bioconjugate Techniques*, Academic Press: San Diego, 1996.

(27) (a) Lee, M. A.; Leslie, D. L. PCT Int. Appl. WO 01/11078, 2001. (b) Lee, M. A.; Brightwell, G. PCT Int. Appl. WO 00/14278, 2000.

(28) (a) Benson, S. C.; Singh, P.; Glazer, A. *Nucleic Acids Res.* **1993**, *21*, 5727. (b) Ferguson, B. Q.; Yang, D. C. H. *Biochemistry* **1986**, *25*, 5298.

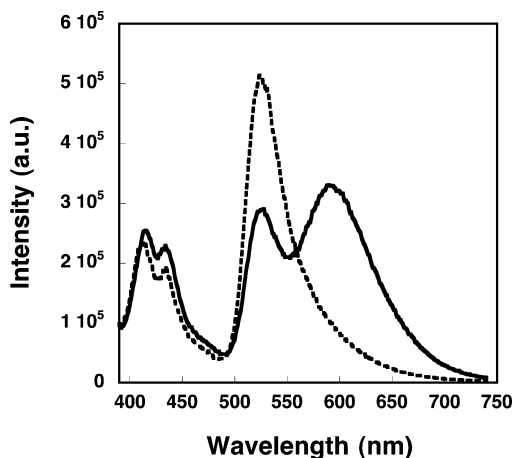
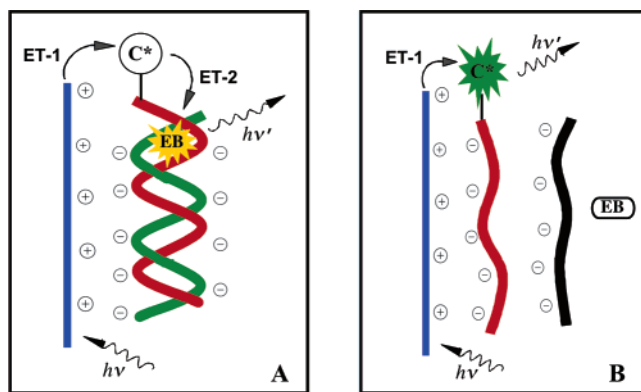


Figure 4. Emission spectra from solutions (solid line) **1**/dsDNA-FI (ssDNA_P-FI + ssDNA_C)/EB and (dotted line) **1**/ssDNA_P-FI + ssDNA_{NC}/EB: $\lambda_{\text{ex}} = 380$ nm; [**1**] = 1.6×10^{-7} M in RUs; [ssDNA_P-FI, ssDNA_C, or dsDNA-FI] = 1.0×10^{-8} M; [EB] = 1.1×10^{-6} M. Measurements are in potassium phosphate–sodium hydroxide buffer solution (50 mM, pH = 7.40).

Scheme 3



From the considerations above, it seemed possible to increase the EB emission by orchestrating electrostatic interactions and optical events, as shown in Scheme 3. One begins with a solution that contains **1**, ssDNA_P-FI, and EB. Situation A shows that addition of a complementary target, ssDNA_C, results in the formation of a double helix, dsDNA-FI (ssDNA_P-FI + ssDNA_C), and the intercalation of EB within the duplex structure. Excitation of **1** leads to energy transfer from **1** to dsDNA-FI (ET-1) and then energy transfer from dsDNA-FI to EB (ET-2). Emission from the intercalating dye EB should be observed only under these circumstances. For situation B, when noncomplementary target ssDNA_{NC} is present, base-pair hybridization does not occur, no EB intercalation is possible, and no EB emission is expected, since the distance between the FI donor and EB acceptor remains too large for effective FRET.

Figure 4 contains spectra that support Scheme 3. Only polymer and fluorescein emission are observed upon excitation of **1** (380 nm) in a mixture containing **1**, ssDNA_P-FI, ssDNA_{NC}, and EB. There is no detectable emission from EB under these conditions, nor is there appreciable emission from FI if a solution of ssDNA_P-FI, ssDNA_{NC}, and EB is excited at 380 nm (i.e., in the absence of **1**). Figure 4 also shows that, in a mixture of **1**,

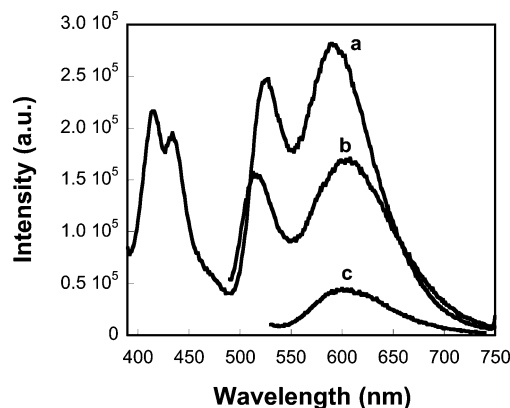


Figure 5. Emission spectra from solutions (a) **1**/dsDNA-FI (ssDNA_P-FI + ssDNA_C)/EB, $\lambda_{\text{ex}} = 380$ nm, (b) dsDNA-FI (ssDNA_P-FI + ssDNA_C)/EB, $\lambda_{\text{ex}} = 480$ nm, and (c) dsDNA (ssDNA_P + ssDNA_C)/EB, $\lambda_{\text{ex}} = 500$ nm; [**1**] = 1.6×10^{-7} M in RUs; [dsDNA-FI or dsDNA] = 1.0×10^{-8} M; [EB] = 1.1×10^{-6} M. Measurements are in potassium phosphate–sodium hydroxide buffer solution (50 mM, pH = 7.40).

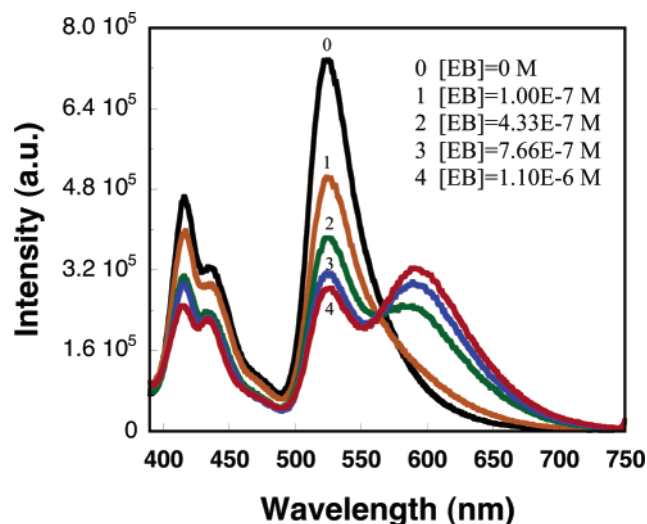


Figure 6. Emission spectra of **1**/dsDNA-FI (ssDNA_P-FI + ssDNA_C)/EB as a function of EB concentration: $\lambda_{\text{ex}} = 380$ nm; [**1**] = 1.6×10^{-7} M in RUs; [dsDNA-FI] = 1.0×10^{-8} M; [EB] from 0 to 1.1×10^{-6} M. Measurements are in potassium phosphate–sodium hydroxide buffer solution (50 mM, pH = 7.40).

dsDNA-FI, and EB, there is strong EB emission upon excitation of **1**.

Comparison of the spectra presented in Figures 3 and 4 indicates that the FI improves the overall energy transfer from **1** to EB. Figure 5 shows that excitation (380 nm) of **1** in a solution of **1**/dsDNA-FI (ssDNA_P-FI + ssDNA_C)/EB results in emission intensities of EB that are ~8-fold greater than that of the directly excited (500 nm) EB/dsDNA (ssDNA_P + ssDNA_C). Direct excitation of FI (480 nm), in the absence of **1**, only provides an approximate 4-fold sensitization of the intercalated EB.²⁴ It is also informative that the overall integrated emission from the acceptor chromophores (FI + EB) is approximately two times larger with the dsDNA-FI structure than that with ssDNA-FI. Altogether, these data show evidence of signal amplification by FRET from **1** to the EB.

Additional experiments optimized the energy transfer by varying the ratio of EB to **1** and dsDNA-FI (ssDNA_P-FI + ssDNA_C). Figure 6 shows that, at concentrations of [dsDNA-FI] = 1.0×10^{-8} M and [**1**] = 1.6×10^{-7} M, additions of EB cause a decrease in the emission intensities of **1** and fluorescein,

(29) Cardullo, R. A.; Agrawal, S.; Flores, C.; Zamecnik, P. C.; Wolf, D. E. *Proc. Natl. Acad. Sci. U.S.A.* **1988**, *85*, 8790.

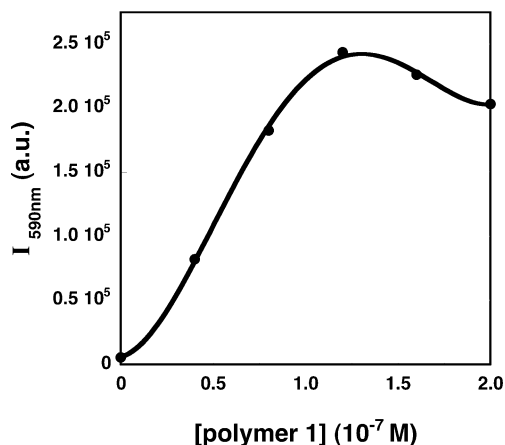


Figure 7. Emission intensity of EB at 590 nm from **1**/dsDNA-FI (ssDNA_P-FI + ssDNA_C)/EB as a function of [**1**]: $\lambda_{\text{ex}} = 380$ nm; [dsDNA-FI] = 1.0×10^{-8} M; [EB] = 1.1×10^{-6} M; [**1**] = from 0 to 2.0×10^{-7} M in RUs. Measurements are in potassium phosphate–sodium hydroxide buffer solution (50 mM, pH = 7.40).

with a concomitant increase in EB emission intensity. Once the concentration ratio of EB to dsDNA-FI reaches approximately 110 (2.75 equiv of EB/(nucleotide base)), the emission intensity of EB no longer increases.

The EB emission intensity was further optimized by varying the ratios of **1** to EB and dsDNA-FI. Figure 7 shows the EB intensity as a function of [**1**]. In this graph, the emission of EB was measured and any residual FI emission was subtracted.²⁴ At a concentrations of [dsDNA-FI] = 1.0×10^{-8} M and [EB] = 1.1×10^{-6} M, initial additions of **1** cause an immediate rise in the emission intensity of EB. Maximum EB emission intensity occurs at a near 0.7:1 charge ratio of **1** relative to dsDNA-FI. We suspect that beyond this point the EB is displaced from dsDNA-FI by electrostatic repulsion between **1** and EB, which has been observed previously upon interaction of cationic polyelectrolytes with dsDNA/EB complexes.^{30,31} The displaced EB is poorly emissive and finds itself too far from dsDNA-FI for efficient FRET.

The proposed energy-transfer mechanism was examined using fluorescence decay kinetics. The fluorescence lifetime measured for **1** in the presence of dsDNA was approximately 240 ps. Unfortunately, this time scale is near our instrument detection limits. Any shortening of the lifetime due to FRET could not be measured with a high degree of accuracy. Instead, we focused on the fluorescence decay of the dsDNA-bound fluorescein upon excitation of **1** with 400 nm laser pulses. The fluorescence lifetime at 520 nm of fluorescein in **1**/dsDNA-FI is approximately 930 ps (Figure 8). Direct excitation of fluorescein at 400 nm does not result in measurable emission; thus any measured emission in **1**/dsDNA-FI solutions is a result of FRET from **1**. For **1**/dsDNA-FI/EB, the lifetime of fluorescein decreases to 315 ps (Figure 8). This decrease in lifetime is due to the efficient FRET from fluorescein to EB and provides unambiguous evidence for the proposed energy-transfer sequence.

Fluorescence anisotropy measurements provide further information on the mechanism of energy transfer. The two

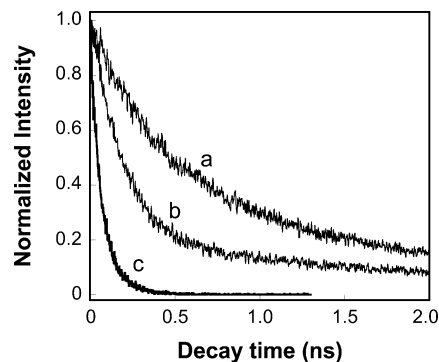


Figure 8. Fluorescence decay of fluorescein recorded at 520 nm for (a) **1**/dsDNA-FI (ssDNA_P-FI + ssDNA_C), (b) **1**/dsDNA-FI (ssDNA_P-FI + ssDNA_C)/EB, and (c) the instrument response function (IRF): $\lambda_{\text{ex}} = 400$ nm; [dsDNA-FI] = 1.0×10^{-7} M; [EB] = 1.1×10^{-5} M; [**1**] = 1.6×10^{-6} M in RUs. Measurements are in potassium phosphate–sodium hydroxide buffer solution (50 mM, pH = 7.40).

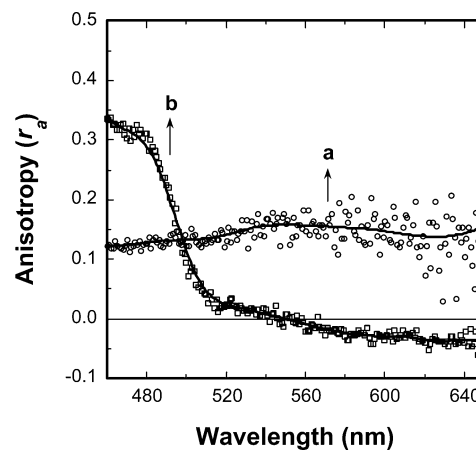


Figure 9. Fluorescence anisotropy of (a) **1**/dsDNA(ssDNA_P + ssDNA_C) and (b) **1**/dsDNA-FI (ssDNA_P-FI + ssDNA_C)/EB as a function of wavelength: $\lambda_{\text{ex}} = 380$ nm; [dsDNA-FI or dsDNA] = 1.0×10^{-8} M; [EB] = 1.1×10^{-6} M; [**1**] = 1.6×10^{-7} M in RUs. Measurements are in potassium phosphate–sodium hydroxide buffer solution (50 mM, pH = 7.40).

predominant mechanisms for loss of anisotropy are rotational motion¹⁸ and energy transfer, either degenerate, among conjugated segments, or to a lower energy site. For a **1**/dsDNA solution, an anisotropy value of 0.12 at 460 nm is observed (Figure 9a). These data do not allow deconvolution of the extent that molecular motion and intrachain energy transfer participate in lowering the initial anisotropy. However, similar anisotropy values have been reported for poly(phenylene ethynylene) derivatives with slow rotational motion and facile intrachain energy migration.³²

The introduction of fluorescein and EB to the interpolyelectrolyte complex, **1**/dsDNA-FI/EB, results in an increase in the measured anisotropy ($r_a = 0.33$ at 460 nm) in the spectral region where **1** is emissive (Figure 9b). Since the presence of FI and EB does not significantly change the size of the complex, we attribute the increase in anisotropy (Figure 9a vs 9b) to the energy-transfer processes from **1** to FI and EB. Energy transfer will result in a decrease in the measured lifetime of the donor chromophore.¹⁸ With decreasing lifetime, processes that can randomize the orientation of the emitting dipoles (i.e. molecular

(30) Izumrudov, V. A.; Zhiryakova, M. V.; Goulko, A. A. *Langmuir* **2002**, *18*, 10348.

(31) Bronich, T. K.; Nguyen, H. K.; Eisenberg, A.; Kabanov, A. V. *J. Am. Chem. Soc.* **2000**, *122*, 8339.

(32) Rose, A.; Lugmair, C. G.; Swager, T. M. *J. Am. Chem. Soc.* **2001**, *123*, 11298.

rotation, intrachain energy transfer, etc.) become less influential.³³

An anisotropy value near zero ($r_a = 0.022$ at 530 nm) is observed in the emission range of fluorescein, consistent with a chromophore that can achieve a random orientation within the lifetime of its excited state. Tethered fluorescein molecules typically have rotational time scales which can be over an order of magnitude faster than their measured lifetime leading to little observable anisotropy.^{33,34} Figure 9b also shows a negative fluorescence anisotropy in the region where EB is emissive (550–650 nm), which implies an angle greater than 54.7° between the transition moments of **1** and EB. This angle corresponds to the situation where the anisotropy equals zero and is often referred to as the “magic angle”.¹⁸

Taken together, the data in Figure 9 are consistent with the proposed two-step energy-transfer mechanism. Indeed, the negative anisotropy (Figure 9b, $\lambda > 550$ nm) strongly suggests that the inefficient transfer from **1** to EB observed in Figure 3 is due to a nonoptimized transition dipole orientation and to a rigid interpolyelectrolyte complex that experiences little rotational freedom within the excited-state lifetimes of the emissive species. The conformational freedom of fluorescein thus serves as a gate for FRET from **1** to the intercalated EB.

Conclusion

In summary, we have shown that it is possible to take advantage of fluorescein attached at a DNA terminus as a fluorescence resonance gate for transferring conjugated polymer excitations to dyes intercalated within dsDNA. Such gate effects are expected for other dyes. Since the net overlap integral between **1** and EB does not change upon Fl attachment to DNA, we suspect that the increased FRET efficiency from **1** to EB is a result of a closer proximity between Fl and **1** and the increased conformational freedom of Fl, relative to EB. We note that both EB and **1** are positively charged, and thus electrostatic repulsion between the two molecules should be expected. EB is wedged within DNA and experiences little independent mobility. Fl, at the end of the dsDNA, can sample multiple orientations within the excited-state lifetime of **1** and can therefore optimize the orientation of its transition moment for FRET with **1**. Once the excitation is located on Fl, a second FRET process, from Fl to EB takes place. The stepwise energy-transfer process provides signal amplification of EB emission by the light-harvesting properties of **1**.

Experimental Section

The oligonucleotides were purchased from Sigma-Genosys (Woodlands, TX). DNA concentrations were determined by measuring the

absorbance at 260 nm in a 200 μ L quartz cuvette. The probe ssDNA_P or ssDNA_P-Fl was mixed with an equal molar amount of the complementary strand ssDNA_C or with a noncomplementary strand ssDNA_{NC} in buffer solution (0.1 M NaCl + 0.01 M sodium citrate). Both complementary and noncomplementary samples were annealed at 2 °C below the melting temperature T_m (58.5 °C) for 25 min and then slowly cooled to room temperature. FRET experiments were done by two ways: (a) the dsDNA or ssDNA_P + ssDNA_{NC} ([dsDNA or ssDNA] = 1.0×10^{-8} M) were mixed with **1** ([**1**] = 1.6×10^{-7} M) at room temperature in the buffer solution, successive additions of EB were performed, and the fluorescence spectra were measured; (b) the dsDNA or ssDNA_P + ssDNA_{NC} ([dsDNA or ssDNA] = 1.0×10^{-8} M) were mixed with EB ([EB] = 1.1×10^{-6} M) at room temperature in a buffer solution, successive additions of **1** were performed, and the fluorescence spectra were measured. The buffer solution was potassium phosphate–sodium hydroxide (50 mM, pH = 7.40). Water was purified using a Millipore filtration system. The synthesis of **1** is available in the literature.²²

The fluorescence anisotropy values (r_a) for **1** and energy-transfer components (fluorescein and EB) were determined by exciting polymer **1** with linearly polarized light and analyzing the depolarization of the fluorescence at different wavelengths corresponding to the respective chromophores (**1**, fluorescein, or EB). Fluorescence measurements used a 3 mL quartz cuvette and a PTI Quantum Master fluorometer equipped with a Xenon lamp excitation source.

Fluorescence lifetime measurements have been performed using a time-correlated single-photon-counting (TCSPC) technique.³⁵ The emission was excited by laser pulses with a wavelength of 400 nm and duration of nearly 120 fs, produced via the second harmonic generation process from the output of an ultrafast Ti:sapphire regenerative amplifier (Spectraphysics Spitfire). The luminescence was dispersed in a spectrometer and detected by a microchannel-plate photomultiplier tube (MCP PMT; Hamamatsu R3809U-51). MCP PMT output and triggering signal from a fast photodiode were connected to a SPC-300 TCSPC board (Beker & Hickl) which performed the statistical analysis of the photon flux and restored the fluorescence transients. TCSPC data were filtered numerically to remove electrical ringing noise and were deconvoluted from the instrument response. Instrument response was measured using the signal generated by a nonluminescent scattering sample at the excitation wavelength.

Acknowledgment. We thank the NIH (Grant GM62958-01) and NSF (Grant DMR-0097611) for support of this work. We also would like to thank Dr. Alexander Michailovsky for his help in the fluorescence lifetime measurements, Dr. Qinghua Xu for his help in performing the fluorescence anisotropy measurements, and Professor Alan Heeger for helpful discussions.

JA035550M

(33) Bene, L.; Fulwyler, M. J.; Damjanovich, S. *Cytometry* **2000**, *40*, 292.

(34) Parkhurst, L. J.; Parkhurst, K. M.; Powell, R.; Wu, J.; Williams, S. *Biopolymers* **2002**, *61*, 180.

(35) O'Connor, D. V.; Phillips, D. *Time Correlated Single Photon Counting*; Academic Press: London, U.K., 1984.